

Cation distributions and possible phase separation in $\text{Tl}_2\text{Ba}_2\text{CuO}_{6+\delta}$ from synchrotron powder x-ray diffraction

M. A. G. Aranda,* D. C. Sinclair,[†] and J. P. Attfield

*Interdisciplinary Research Centre in Superconductivity, University of Cambridge,
Madingley Road, Cambridge CB3 0HE, United Kingdom*

and Department of Chemistry, University of Cambridge, Lensfield Road, Cambridge CB2 1EW, United Kingdom

A. P. Mackenzie

*Interdisciplinary Research Centre in Superconductivity and Department of Physics, Cavendish Laboratory,
University of Cambridge, Madingley Road, Cambridge CB3 0HE, United Kingdom*

(Received 6 October 1994; revised manuscript received 18 January 1995)

Orthorhombic and tetragonal $\text{Tl}_2\text{Ba}_2\text{CuO}_{6+\delta}$ (Tl-2201) samples have been studied using resonant synchrotron x-ray powder diffraction data at energies just below the Cu K and Tl L_{III} absorption edges. The resonant contributions enable us to demonstrate that Cu substitutes at the Tl site; the tetragonal structure is stabilized by a higher (5.5%) degree of substitution than the orthorhombic (< 1%) material, in excellent agreement with electron probe microanalysis results. A slight splitting of some diffraction peaks of oxygen-rich orthorhombic Tl-2201 is consistent with a phase separation due to the segregation of interstitial oxygens.

I. INTRODUCTION

$\text{Tl}_2\text{Ba}_2\text{CuO}_{6+\delta}$ (Fig. 1) is the first member of the $\text{Tl}_2\text{Ba}_2\text{Ca}_{n-1}\text{Cu}_n\text{O}_{4+2n+\delta}$ series of copper-oxide superconductors containing double TlO layers. It contains single CuO_2 planes ~ 11.6 Å apart and has proved to be one of the most important copper-oxide materials for physical measurements. Kubo and co-workers showed that it is possible to depress T_c from 90 to below 4 K by the addition of oxygen,^{1,2} giving an excellent opportunity to study the overdoped side of the superconducting phase diagram. Studies of the transport properties of high-quality single crystals have shown that the resistivity evolves smoothly from a linear to a quadratic temperature dependence as the doping is increased.³ As T_c is lowered by overdoping, the critical magnetic field scale is rapidly reduced, allowing the normal state to be studied down to mK temperatures.⁴ These measurements give direct evidence that the residual resistivity is very low (~ 5 – 10 $\mu\Omega$ cm) in the best samples, confirming the importance of Tl-2201 for studies of the intrinsic properties of copper-oxide superconductors.

There is, however, significant variation in the chemical and structural properties of Tl-2201. All of the detailed single-crystal studies of transport and magnetic properties have been carried out on tetragonal samples, although orthorhombic Tl-2201 is also known. Shimakawa showed that a similar range of physical properties can be accessed in both forms by oxygen doping.⁵ He proposed that the variation in crystallographic symmetry of Tl-2201 is due to the degree of substitution of Cu for Tl, high levels of substitution being necessary to stabilize the tetragonal form, based on the differences in starting composition needed to produce each form, and differences in the Curie term of their normal-state magnetic susceptibilities.

In this paper, we have used two independent techniques to obtain accurate chemical analyses of tetragonal and orthorhombic Tl-2201 powders.⁶ Electron probe microanalysis (EPMA) provides the overall cation ratios in these materials,⁷ and resonant powder x-ray diffraction gives a site-by-site chemical analysis by using monochromatic x rays at energies just below an elemental absorption edge. This gives rise to large anomalous dispersion corrections to the atomic scattering factor of the given element, from which the distribution of that ele-

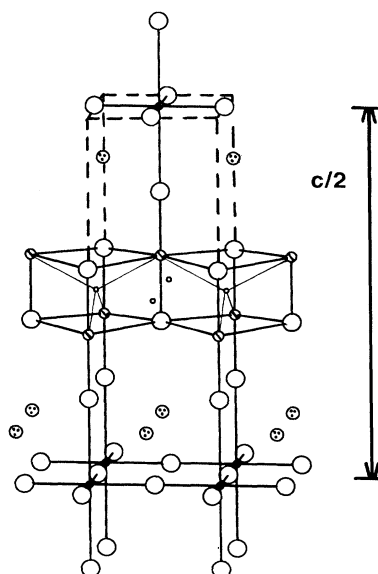


FIG. 1. The tetragonal Tl-2201 structure (Cu, solid; Tl, hatched; Ba, speckled; lattice O, large open; and interstitial O, small open circles). Cu-O and Tl-O bonds including those to interstitial sites are shown.

ment over symmetry inequivalent sites within a disordered crystal structure is determined.^{8,9} Distributions of several elements are found through the simultaneous analysis of data collected at the absorption edges of the relevant elements. This method has recently been used to show that the cation disorder at each site in (Tl,Pb)-1223 [(Tl_{0.5}Pb_{0.5})Sr₂Ca₂Cu₃O₉] and Tl-2223 (Tl₂Ba₂Ca₂Cu₃O₁₀) superconductors is (Tl,Pb)(Sr,Ca)₂(Ca,Tl)₂Cu₃O₉ (Ref. 10) and (Tl,Cu)₂Ba₂(Ca,Tl)₂Cu₃O₁₀,¹¹ respectively. The highly resolved synchrotron diffraction data also yield structural information such as the effects of interstitial oxygen, and our data reveal a possible oxygen phase separation in orthorhombic Tl-2201.

II. EXPERIMENTAL DETAILS

Tl-2201 samples were prepared using high-purity powders of Tl₂O₃ (99.99%), BaO₂ (98%), and CuO (99.999%), with the CuO being dried overnight at 700°C prior to use. Six charges (~0.9 g each) were individually mixed into a paste with acetone using an agate mortar and pestle for 30 min and then pressed into pellets (10×3 mm) under a pressure of 5 ton/cm². The pellets were wrapped in gold foil envelopes during the various heating cycles to reduce the loss of thallium at elevated temperatures. This grinding and pelleting procedure was repeated for subsequent heating cycles. Samples were cooled after the reaction period to 25°C at 10°C/min, under flowing oxygen throughout. The starting composition for the tetragonal Tl-2201 phase was Tl:Ba:Cu = 2.10:2.00:1.15 and the heating steps were: 800°C (10 h), 820°C (10 h), 865°C (5 h), 865°C (3 h). The orthorhombic sample had starting composition Tl:Ba:Cu = 2.10:2.00:1.06 and reaction profile 800°C (10 h), 820°C (10 h).

The samples were characterized by ac susceptibility, dc resistivity, electron probe microanalysis (EPMA), and resonant synchrotron x-ray powder diffraction. The ac magnetic susceptibility was recorded using a Lake Shore 7000 susceptometer with a frequency of 333 Hz and an applied magnetic field of 1 Oe. The standard four-point probe method, with an applied current of 1 mA, was used for dc electrical resistivity measurements on a sintered bar.

The EPMA study was carried out using a Cameca SX-50 electron microprobe equipped with both wavelength and energy dispersive spectrometers. The samples were embedded in conducting epoxy and polished using 1-μm diamond paste. X-ray mapping was carried out over a wide area (~1 mm²) using the energy dispersive spectrometer to check for secondary phases. More accurate analyses of the stoichiometry of the 2201 grains were performed using the wavelength dispersive spectrometers. The grain sizes were sufficient (>10 μm) to allow analyses of a series of individual grains from each specimen as a test of overall homogeneity. All four elements were studied, using the Tl L_α, Ba L_α, Cu K_α, and O K_α x-ray lines. The standards were single crystals of YBa₂Cu₃O₇ (small oxygen nonstoichiometry and Al contamination were taken into account) and a previously characterized Tl-2201 sample.¹² The measured grain-to-grain variation

of the cations was ~1%, consistent with experimental error for this kind of sample. Analytical accuracy for the cations, whose x rays are not prone to severe absorption effects, was about 1–2 %, but for oxygen this was degraded to 3–4 % due to the effect of surface topology (surface rounding of the polished grains, for example) on the degree of x-ray absorption. At this level of accuracy the oxygen results do not give useful information on the small deviations from stoichiometry that are present in these materials.

The resonant synchrotron x-ray powder diffraction study of the as-prepared materials was carried out on diffractometer 2.3 at the EPSRC Synchrotron Radiation Source, Daresbury, UK. For each sample, two resonant diffraction patterns at energies just below the Tl L_{III} and Cu K absorption edges were collected. The experimental conditions were the following.

(i) Tl L_{III} edge patterns. λ = 0.979 66(3) Å, 12 eV below the Tl³⁺ L_{III} edge. (a) Tetragonal Tl-2201, 2θ = 12°–96°, 0.01° steps, 4 s counting time. (b) Orthorhombic Tl-2201, 2θ = 12°–91°, 0.01° steps, 3 s counting time.

(ii) Cu K edge patterns. λ = 1.381 81(3) Å, 10 eV below the Cu²⁺ K edge. (a) Tetragonal Tl-2201, 2θ = 12°–120°, 0.02° steps, 6 s counting time. (b) Orthorhombic Tl-2201, 2θ = 12°–120°, 0.02° steps, 4 s counting time.

The wavelengths were selected and calibrated using NIST Si powder as standard (*a* = 5.430 94 Å). The *f'* values were calculated using the program FPRIME,¹³ allowing for valence shifts in the absorption edge positions which were taken from published x-ray absorption near-edge structure (XANES) spectra.^{14,15} The profiles were fitted by the Rietveld method¹⁶ using the generalized structure analysis system (GSAS) (Ref. 17) package. The diffraction peaks were fitted by a numerical convolution of Gaussian and Lorentzian functions with full widths at half maximum (FWHM) Γ_G and Γ_L given by^{18,19}

$$\Gamma_G = (U \tan^2 \theta + V \tan \theta + W)^{1/2},$$

$$\Gamma_L = (X + X' \cos \phi) \tan \theta + (Y + Y' \cos \phi) / \cos \theta.$$

In the latter expression, the *X* and *Y* terms allow for Scherrer (particle size) and strain broadening, respectively. Anisotropy may be modeled by the *X'* and *Y'* terms, where *φ* is the angle between a chosen principal axis and the reciprocal-lattice vector of the Bragg reflection.

III. RESULTS

The ac magnetic susceptibility measurements for the as-prepared orthorhombic and tetragonal Tl-2201 samples showed no superconducting transitions down to 4.2 K. However, when a small bar of the tetragonal sample was post-annealed in Ar at 480°C for 5 h and quenched into liquid N₂, dc resistivity measurements revealed a sharp resistive transition with *T_c*(0) = 49 K.

The EPMA study using the energy dispersive spectrometer revealed no impurities in the tetragonal Tl-2201 sample, but in the orthorhombic specimen a little CuO (<0.5% by volume) was detected. The mean Tl:Ba:Cu ratios were 1.89:1.99:1.12 for the tetragonal sample and

TABLE I. Final structural parameters for tetragonal Tl-2201, in space group $I4/mmm$. Overall R factors (%): $R_{WP}=6.9$, $R_P=4.9$, $R_F=7.7$. Cell data: $a=3.86409(2)$ Å, $c=23.1372(1)$ Å, $V=345.466(4)$ Å³.

FWHM							
parameters	Gaussian (0.01°) ²				Lorentzian (0.01°)		
Profile	U	V	W	X	X'	Y	Y'
Tl L_{III} edge	71(6)	−31(4)	9.6(6)	0.95(5)	0	6.4(2)	−1.8(1)
Cu K edge	56(4)	−26(4)	10.7(9)	1.69(7)	0	4.4(2)	−2.6(1)
Atom	Position	x	y	z	U_{iso} (Å ²)	Occupancy	
Tl	16m	0.524 5(5)	0.524 5	0.202 88(3)	0.000 9(5)	0.236(1)	
Cu(Tl)	4e	0.5	0.5	0.219(2)	0.0009	0.056	
Ba	4e	0	0	0.08439(3)	0.0009	1.0	
Cu	2b	0.5	0.5	0	0.0009	1.0	
O(1)	4c	0	0.5	0	0.003(2)	1.0	
O(2)	4e	0.5	0.5	0.1156(3)	0.006(2)	1.0	
O(3)	16m	0.579(3)	0.579	0.2922(4)	0.011(5)	0.25	
O(4)	4d	0	0.5	0.25	0.011	0.090(15)	

1.97:2.02:1.01 for the orthorhombic material, using the wavelength dispersive spectrometer. The resonant diffraction study gave the following results.

A. Tetragonal Tl-2201

The x-ray powder diffraction patterns show no impurity lines, in agreement with the EPMA results. The sharp Bragg peaks were indexed on a tetragonal unit cell [space group $I4/mmm$, $a=3.68412(2)$ Å, $c=23.1375(1)$ Å]. The Rietveld refinement was carried out using the structure reported by Kolesnikov *et al.*² as a starting model. Disorder of Tl and O(3) in the xy plane was modeled by refining them off their ideal ($\frac{1}{2}, \frac{1}{2}, z$) sites onto (x, x, z) positions, following the work of Dmowski *et al.*²⁰ who found displacements along $[110]$ using pair distribution functions derived from neutron-diffraction data for the related compound $Tl_2Ba_2CaCu_2O_8$. The proposed Cu substituent at the Tl site, atom Cu(Tl) was refined on ($\frac{1}{2}, \frac{1}{2}, z$), following previous models for Tl-2201 (Ref. 2) and Tl-2223 (Ref. 11) structures. The peak broadening was found to be principally Lorentzian, and a slight anisotropy was best fitted by refinement of the Y' parameter, assuming the principal strain axis to be $[001]$.

The structural model was fitted to both synchrotron diffraction profiles simultaneously to make use of the difference in scattering factor for Tl and Cu between the two patterns due to the resonant contributions. This enabled the occupation factors of Tl and Cu(Tl) to be refined independently, giving values of 0.936(8) and 0.052(16), respectively. The overall Tl site occupancy of 0.988(18) clearly indicates that no significant cation vacancy formation occurs, so in the final refinements the Tl and Cu occupancies were constrained to sum to 1.0. Refinement of the occupation factor for the excess oxygen site between the TlO planes, O(4), gave a value of 0.09(1). The final refined composition is $(Tl_{1.89(1)}Cu_{0.11(1)})Ba_2CuO_{6.18(3)}$. Results of the final refinement are given in Table I and the profile plots are displayed in Fig. 2.

B. Orthorhombic Tl-2201

All of the diffraction peaks observed in the resonant synchrotron x-ray powder patterns could be assigned to the orthorhombic 2201 phase, and the fundamental peaks were indexed on an orthorhombic unit cell [$a=5.4480(1)$ Å, $b=5.4969(1)$ Å, and $c=23.1780(2)$ Å]. The ob-

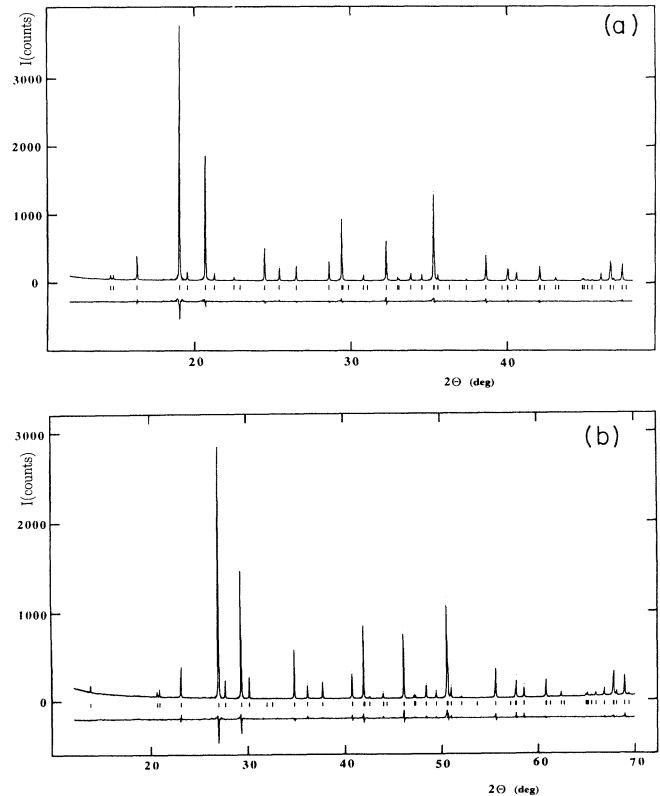


FIG. 2. Observed, calculated, and difference plots for tetragonal Tl-2201 using synchrotron x-ray wavelengths of (a) 0.98 and (b) 1.38 Å. Reflection positions are marked.

served systematic absences are consistent with space group $Fmmm$ as reported elsewhere.^{5,21} Additional satellite peaks due to an incommensurate structural modulation were also observed (Fig. 3). These have previously been reported from x-ray, neutron-, and electron-diffraction studies of oxygen-rich samples,^{5,22,23} and have reciprocal-lattice vectors given by

$$\mathbf{d}^*(hklm)_{\pm} = (h \pm mq_x)\mathbf{a}^* + (k + mq_y)\mathbf{b}^* + (l + mq_z)\mathbf{c}^*,$$

where h , k , l , and m are integers, \mathbf{a}^* , \mathbf{b}^* , and \mathbf{c}^* are the reciprocal cell vectors, and the propagation vector is $\mathbf{q} = \langle \pm q_x, q_y, q_z \rangle$.

Using the previously reported values of $\langle \pm 0.07, 0.22, 1 \rangle$ for \mathbf{q} ,⁵ the satellites were indexed and the variable components were refined from the positions of five well-resolved peaks. The indexing is presented in Table II and the refined propagation vector was $\langle \pm 0.046(1), 0.217(1), 1 \rangle$. The intensity of the strongest 0201_{\pm} satellite peak was <2% that of the most intense 115 fundamental reflection, so the average structure was fitted as described below, neglecting the satellite reflections.

The Rietveld refinement of the average orthorhombic Tl-2201 structure was carried out using the structure reported by Parise *et al.* as a starting model.²¹ A marked anisotropic peak broadening was observed, and this was successfully modeled by refinement of the Lorentzian strain terms Y and Y' in addition to the three Gaussian parameters, with the principal strain axis again taken to be $[001]$. This fit of a single orthorhombic Tl-2201 phase to the data gave a fair agreement between observed and calculated profile intensities (overall R_{wp} for the two-pattern refinement = 8.7%). However, careful examination of the profile revealed slight splittings of some diffraction peaks, e.g., 040 (Fig. 4), that were inconsistent with this model. These could not be fitted as a lattice distortion lowering the crystal symmetry to monoclinic or triclinic, but were found to be consistent with the presence of two orthorhombic phases (hereafter referred to as Ortho1 and Ortho2) differing in their a and b cell parameter values. The two phases were fitted to the profile by independently varying their scale factors and lattice constants while their peak width and atomic parameters

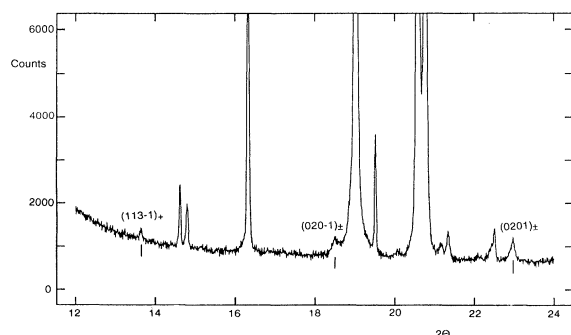


FIG. 3. Expanded section of the 0.98 Å diffraction pattern of orthorhombic Tl-2201 with superstructure peaks labeled.

TABLE II. Results of the indexing of the incommensurate peaks using the propagation vector $\langle \pm 0.046(1), 0.217(1), 1 \rangle$.

$hklm + / -$	d_{obs} (Å)	d_{calc} (Å)
113-1 ₊	4.1380	4.1378
020-1 _±	3.0544	3.0548
0201 _±	2.4642	2.4647
131-1 ₊	1.8664	1.8665
311-1 ₊	1.7830	1.7835

were constrained to be the same. This resulted in a significant decrease in the overall R_{wp} for the joint refinement to 7.9%. Disorder in the TlO planes was modeled by refining anisotropic thermal parameters or displacement for Tl and O(3). It was found that the disorder of both these atoms is parallel to \mathbf{b} , and no significant displacements parallel to \mathbf{a} were found, in agreement with a previous powder neutron study.²¹

To discover any compositional differences between Ortho1 and Ortho2, the Tl/Cu ratios at their Tl sites were varied independently, but a significant (>1%) substitution of Cu at the Tl site was not found for either phase. However, independent refinement of the occupation factors for the interstitial oxygen site O(4) gave values of -0.03(7) and 0.16(5) for Ortho1 and Ortho2, respectively, suggesting that the two phases differ in their excess oxygen contents. The value for Ortho1 was fixed at zero in the final refinement, giving the results in Table II and the profile plots displayed in Fig. 5.

IV. DISCUSSION

The EPMA and resonant x-ray-diffraction analyses of the cation contents of tetragonal and orthorhombic Tl-2201 are in excellent agreement. They confirm that the deficiency of Tl in this compound is due to copper substitution [i.e., $(\text{Tl}_{2-x}\text{Cu}_x)\text{Ba}_2\text{CuO}_{6+\delta}$] rather than thallium-site vacancy formation $(\text{Tl}_{2-x}\text{Ba}_2\text{CuO}_{6+\delta})$. The difference between orthorhombic and tetragonal samples lies in the degree of copper substitution, as proposed by Shimakawa.⁵ The orthorhombic sample has $x < 0.02$, whereas the tetragonal sample has $x = 0.11$. The excess

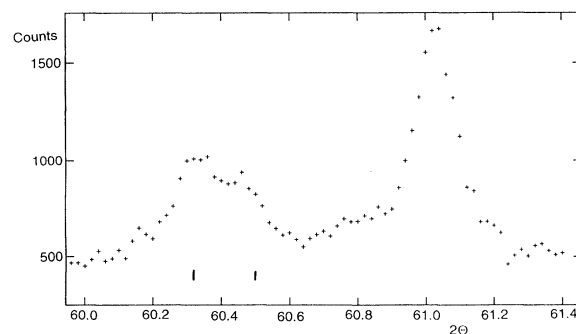


FIG. 4. Part of the 1.38 Å orthorhombic Tl-2201 diffraction data showing a splitting of the 040 peak at 60.4° 2θ . The 040 reflection bars are calculated from the two-phase fit to the entire profile.

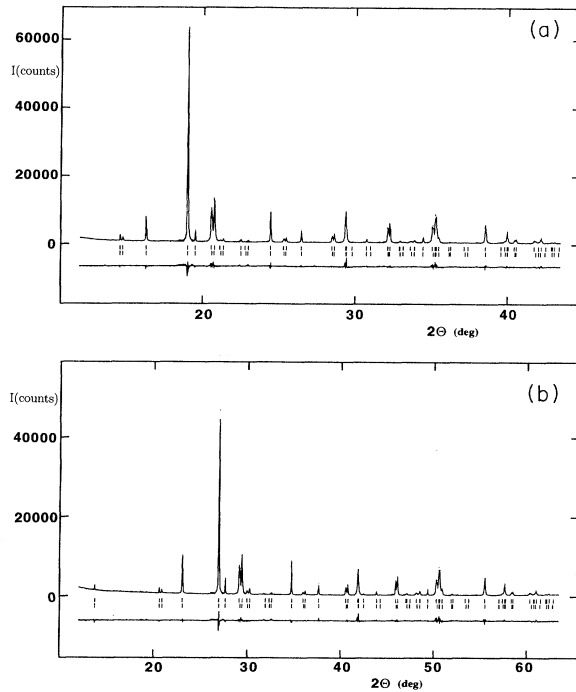


FIG. 5. Observed, calculated, and difference plots for orthorhombic Tl-2201 using synchrotron x-ray wavelengths of (a) 0.98 and (b) 1.38 Å. Reflection positions for the two phases are marked.

oxygen contents of the tetragonal [$\delta=0.18(3)$] and orthorhombic [mean $\delta=0.16(3)$] samples, both prepared under 1 bar oxygen, appear to be insensitive to x . The hole doping of the copper-oxide planes is achieved both by the substitution of Cu^+ or Cu^{2+} for Tl^{3+} and by the intercalation of excess oxygen between the TlO planes.

The orthorhombic to tetragonal transition of Tl-2201

may be described as an order-disorder transition similar to that in $\text{YBa}_2\text{Cu}_3\text{O}_{6+x}$, and results in similar microstructures such as twinned or tweedlike arrangements.^{22,23} At ambient pressures, the transition requires a change of chemical composition, such as thallium loss due to prolonged heating, which may be reversed by the action of Tl_2O_3 on orthorhombic Tl-2201.⁵ Loss of orthorhombicity can also be induced by the creation of oxygen vacancies in the TlO planes.²⁴

The fit to the tetragonal Tl-2201 profiles reveals no evidence of orthorhombic splittings, although a slight anisotropic strain broadening of the Bragg peaks is evident. The mean value of Y' from the fits to the two profiles is equivalent to an excess strain of 0.03% in the xy plane over that in the z direction. The coordinates of the refined model for tetragonal Tl-2201 are similar to those reported elsewhere.² The resonant contributions give a precise Tl/Cu analysis at the Tl site, and it is also possible to refine the occupancy of the interstitial O(4) site due to the high site symmetry and the good resolution and peak to background ratio obtained with the synchrotron x-ray source. The overall composition $(\text{Tl}_{1.89(1)}\text{Cu}_{0.11(1)})\text{Ba}_2\text{CuO}_{6.18(3)}$ leads to a mean Cu oxidation state of +2.4, assuming all the Tl to be trivalent, consistent with the as-prepared material being too overdoped to superconduct. Removal of some of the excess oxygen to reduce the hole doping results in a 49 K superconducting transition.

The fits to the resonant x-ray-diffraction profiles of the orthorhombic Tl-2201 sample were complicated by the presence of an incommensurate modulation, strong anisotropic peak broadening and the apparent phase separation. Comparison of the FWHM parameters in Tables I and III shows that the isotropic Gaussian and Lorentzian strain broadening are more pronounced in the orthorhombic material and a greater anisotropy in the latter term is also present, corresponding to an excess strain of

TABLE III. Final structural parameters for orthorhombic Tl-2201, in space group $Fmmm$. Overall R factors (%): $R_{\text{WP}}=8.2$, $R_p=5.6$, $R_F(\text{Ortho1})=9.2$, $R_F(\text{Ortho2})=9.5$. Scale factors: Ortho1=0.444(7), Ortho2=0.556. Overall $U_{\text{iso}}=0.0040(2) \text{ \AA}^2$.

Cell data	a (Å)		b (Å)		c (Å)		V (Å ³)
Ortho1	5.4513(2)		5.4882(2)		23.1773(7)		693.42(3)
Ortho2	5.4450(1)		5.5030(1)		23.1776(5)		694.49(2)
FWHM							
parameters	Gaussian (0.01°) ²				Lorentzian (0.01°)		
Profile	U	V	W	X	X'	Y	Y'
Tl L_{III} edge	320(40)	−110(20)	23(3)	0	0	26.5(3)	−16.2(3)
Cu K edge	220(30)	−90(20)	26(4)	0	0	26.9(3)	−18.1(4)
Atom	Position	x	y	z	Occupancy		
Tl	16 <i>m</i>	0	0.029 3(4)	0.202 76(4)	0.50		
Ba	8 <i>i</i>	0.5	0	0.08406(4)	1.0		
Cu	4 <i>a</i>	0	0	0	1.0		
O(1)	8 <i>e</i>	0.25	0.75	0	1.0		
O(2)	8 <i>i</i>	0	0	0.1165(4)	1.0		
O(3)	16 <i>m</i>	0	0.065(2)	0.2900(4)	0.50		
O(4)	8 <i>f</i>	0.25	0.25	0.25	0	Ortho1	
					0.15(3)	Ortho2	

0.30% in the xy plane. This may reflect the strain caused by the intergrown domains of the two orthorhombic phases, and is approximately equal to the difference between the spontaneous strains $[2(b-a)/(b+a)]$ of 0.68% in Ortho1 and 1.06% in Ortho2.

The two-phase behavior of the orthorhombic $\text{Ti}_2\text{Ba}_2\text{CuO}_{6+\delta}$ sample is reminiscent of phase-separated $\text{La}_2\text{CuO}_{4+\delta}$.²⁵ In the latter system, oxygen phase separation occurs below 415 K, and the miscibility gap extends from $\delta=0.01$ to 0.055.²⁶ The oxygen-rich $\text{La}_2\text{CuO}_{4+\delta}$ phase has a greater cell volume and orthorhombicity than the $\delta\approx 0$ component, and may show a modulated superstructure due to the ordering of interstitial oxygens. Similar differences are found in our results for the $\text{Ti}_2\text{Ba}_2\text{CuO}_{6+\delta}$ phases (Table III). Ortho2 has $\delta\approx 0.3$, although the accuracy of this value is low with x-ray refinement, and has a larger unit cell and orthorhombicity than Ortho1 for which $\delta\approx 0$. The observed satellite peaks may be assigned to an ordered superstructure of the excess oxygen atoms in Ortho2. The c parameters of Ortho1 and Ortho2 do not differ significantly, suggesting that domains of the two phases are intergrown within the same crystallites. Electron microscopy has previously revealed $\sim 200\times 200\times 800$ Å domains twinned principally on $\{110\}$.²³

Independent evidence for two-phase behavior in oxygen-rich orthorhombic Ti-2201 is provided by the Cu-NQR spectra of four samples reported by Shimakawa.⁵ Random insertion of interstitial oxygen atoms between the TlO layers in Ti-2201 results in displacements of oxygen atoms bonded apically to the CuO_2 planes, which broadens the Cu-NQR resonance. Hence, a tetragonal superconducting Ti-2201 samples with $\delta\approx 0$ displayed a relatively sharp resonance, whereas that for an overdoped nonsuperconducting sample with $\delta\approx 0.1$ was considerably broadened. A similar broad signal was seen for an orthorhombic sample with $\delta\approx 0.1$ although this material has $T_c = 85$ K. However, the most oxygen-rich orthorhombic sample with $\delta\approx 0.25$ in which T_c was depressed to 10 K showed two well-defined Cu resonances. This can be interpreted as evidence for separation into two phases, one with $\delta\approx 0$, and the other with an ordered superstructure of oxygen interstitials, both giving sharp Cu-NQR resonances characteristic of well-defined Cu environments.

The above diffraction and NQR results suggest that a phase separation driven by segregation of the excess interstitial oxygen atoms may occur in orthorhombic $\text{Ti}_2\text{Ba}_2\text{CuO}_{6+\delta}$, analogous to that in $\text{La}_2\text{CuO}_{4+\delta}$. Further high-resolution diffraction and NMR or NQR experiments as a function of temperature will be required to test this hypothesis and accurately determine the limits of any miscibility gap in orthorhombic Ti-2201. Transport and magnetic studies will also be needed to establish the relationship between the miscibility gap and superconducting region. A notable difference is that our apparently phase-separated sample is nonsuperconducting above 4 K, whereas the oxygen-rich component of phase-separated $\text{La}_2\text{CuO}_{4+\delta}$ has $T_c \sim 40$ K. Studies of orthorhombic Ti-2201, in comparison with those on $\text{La}_2\text{CuO}_{4+\delta}$, will help to determine whether the spontane-

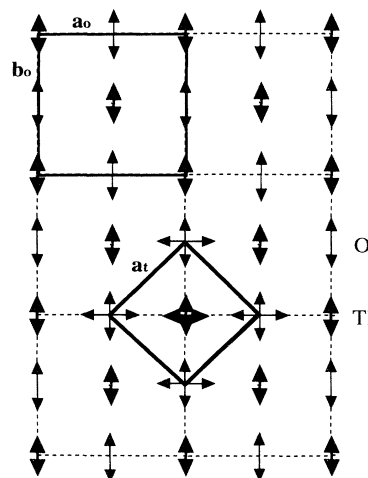


FIG. 6. The relationship between orthorhombic (o) and tetragonal (t) axes for Ti-2201 with displacements of Tl and O(3) in the TlO planes shown for each symmetry.

ous segregation of excess oxygen in these materials is due only to a structural instability, arising from the local strains induced by random oxygen interstitials, or whether an electronic instability associated with superconductivity is also involved.

Orthorhombic Ti-2201 provides a good opportunity to study the local structure of the TlO planes in the $\text{Ti}_2\text{Ba}_2\text{Ca}_{n-1}\text{Cu}_n\text{O}_{4+2n}$ series of superconductors, due to the low crystallographic symmetry and the absence of Cu substitution at the Tl sites. Radial distribution functions derived from pulsed neutron-scattering experiments on tetragonal Ti-2212 have led to a model in which Tl atoms are displaced from their ideal sites in the $[110]_t$ direction and neighboring oxygen atoms are displaced in the perpendicular $[\bar{1}10]_t$ direction,²⁰ resulting in two short Tl-O bonds in the TlO plane (t and o subscripts refer to the tetragonal and orthorhombic axes, see Fig. 6). However, this synchrotron study and a previous powder neutron-diffraction refinement²¹ show that in orthorhombic Ti-2201, the principal displacements of both the Tl and O atoms are parallel to the same $[010]_o$ ($[110]_t$) direction. The model in Fig. 7 derived from our refined coordinates is consistent with both the orthorhombic and tetragonal structures. Well-ordered $\text{O} \cdots \text{Tl-O} \cdots$ chains with al-

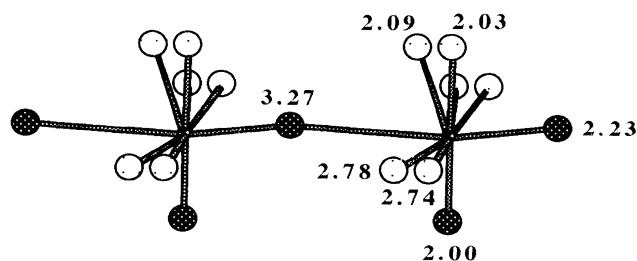


FIG. 7. The proposed chains of TlO_6 octahedra parallel to b in orthorhombic Ti-2201 with Tl-O distances in Å shown for the Tl atom on the right. The lightly speckled O atoms correspond to the two possible orientations of neighboring chains.

ternate short and long Tl-O bonds are formed in the $[010]_o$ direction, but the correlations between the displacements in neighboring chains are too weak to give rise to long range order. Tl is found in a range of distorted octahedral environments, which gives bond valence sums of 2.90–3.09 for Tl, using parameters recently derived for Tl_2O_3 .²⁷

In conclusion, we have confirmed that the tetragonal and orthorhombic forms of Tl-2201 ($\text{Tl}_{2-x}\text{Cu}_x\text{Ba}_2\text{CuO}_{6+\delta}$) differ in cation composition (x) using the two independent analytical techniques of resonant x-ray diffraction and electron probe microanalysis.

The powder diffraction study also gives evidence for a possible phase separation of excess oxygen in the orthorhombic form.

ACKNOWLEDGMENTS

We thank J. M. Wade for performing the resistivity measurements, and D. Laundry for assistance with synchrotron data collection. SRS beam time was provided by EPSRC. M.A.G.A. acknowledges the European Community and A.P.M. acknowledges the Royal Society for financial support.

*Present address: Departamento de Química Inorgánica, Universidad de Málaga, 29071 Málaga, Spain.

†Present address: Department of Chemistry, University of Aberdeen, Aberdeen AB9 2UE, UK.

¹Y. Kubo, Y. Shimakawa, T. Manaho, and H. Igarashi, *Phys. Rev. B* **43**, 7875 (1991).

²There is one report of $T_c = 110$ K in Ca-containing tetragonal Tl-2201 crystals; N. N. Kolesnikov, V. E. Korotkov, M. P. Kulakov, R. P. Shibaeva, V. N. Molchanov, R. A. Tamazyan, and V. I. Simonov, *Physica C* **195**, 219 (1992).

³T. Manaho, Y. Kubo, and Y. Shimakawa, *Phys. Rev. B* **46**, 11 019 (1992).

⁴A. P. Mackenzie, S. R. Julian, G. G. Lonzarich, A. Carrington, S. D. Hughes, R. S. Liu, and D. C. Sinclair, *Phys. Rev. Lett.* **71**, 1238 (1993).

⁵Y. Shimakawa, *Physica C* **204**, 247 (1993).

⁶Some preliminary crystallographic results have been reported in J. P. Attfield, M. A. G. Aranda, and D. C. Sinclair, *Physica C* **235-240**, 965 (1994).

⁷For a recent review see A. P. Mackenzie, *Rep. Prog. Phys.* **56**, 557 (1993).

⁸G. H. Kwei, R. B. Von Dreele, A. Williams, J. Goldstone, A. C. Lawson, II, and W. K. Warburton, *J. Mol. Struct.* **223**, 384 (1990).

⁹J. P. Attfield, *NIST Spec. Publ.* **846**, 175 (1992).

¹⁰M. A. G. Aranda, D. C. Sinclair, and J. P. Attfield, *Physica C* **221**, 304 (1994).

¹¹D. C. Sinclair, M. A. G. Aranda, J. P. Attfield, and J. Rodriguez-Carvajal, *Physica C* **225**, 307 (1994).

¹²R. S. Liu, S. D. Hughes, R. A. Angel, T. P. Hackwell, A. P. Mackenzie, and P. P. Edwards, *Physica C* **198**, 203 (1992).

¹³D. T. Cromer, *J. Appl. Crystallogr.* **16**, 437 (1983).

¹⁴J. B. Parise, P. L. Gai, M. A. Subramian, J. Gopalakrishnan, and A. W. Sleight, *Physica C* **159**, 245 (1989).

¹⁵F. Studer, D. Bourgault, C. Martin, R. Retoux, C. Michel, B. Raveau, E. Dartyge, and A. Fontaine, *Physica C* **159**, 609 (1989).

¹⁶H. M. Rietveld, *J. Appl. Crystallogr.* **2**, 65 (1969).

¹⁷A. C. Larson and R. B. Von Dreele (unpublished).

¹⁸C. J. Howard, *J. Appl. Crystallogr.* **15**, 615 (1982).

¹⁹P. Thompson, D. E. Cox, and J. B. Hasting, *J. Appl. Crystallogr.* **20**, 79 (1987).

²⁰W. Dmowski, B. H. Toby, T. Egami, M. A. Subramanian, J. Gopalakrishnan, and A. W. Sleight, *Phys. Rev. Lett.* **61**, 2608 (1988).

²¹J. B. Parise, C. C. Torardi, M. A. Subramanian, J. Gopalakrishnan, A. W. Sleight, and E. Prince, *Physica C* **159**, 239 (1989).

²²R. Beyers, S. S. P. Parkin, V. Y. Lee, A. I. Nazzari, R. Savoy, G. Gorman, T. C. Huang, and S. LaPlaca, *Appl. Phys. Lett.* **53**, 432 (1988).

²³E. A. Hewat, P. Bordet, J. J. Capponi, C. Chaillout, J. Chénavas, M. Godinho, A. W. Hewat, J. L. Hodeau, and M. Marezio, *Physica C* **156**, 375 (1988).

²⁴C. Opagiste, G. Triscone, M. Couach, T. K. Jondo, J.-L. Jorda, A. Junod, A. F. Khoder, and L. Muller, *Physica C* **213**, 17 (1993).

²⁵See references in *Phase Separation in Cuprate Superconductors*, edited by K. A. Muller and G. Benedek (World Scientific, Singapore, 1993).

²⁶P. G. Radaelli, J. D. Jorgensen, R. Kleb, B. A. Hunter, F. C. Chou, and D. C. Johnston, *Phys. Rev. B* **49**, 6239 (1994).

²⁷H. H. Otto, R. Baltrusch, and H.-J. Brandt, *Physica C* **215**, 205 (1993).